Local equilibrium hypothesis and Taylor's dissipation law

2016 Fluid Dyn. Res. 48 021402

(http://iopscience.iop.org/1873-7005/48/2/021402)

IOP Publishing | The Japan Society of Fluid Mechanics Fluid *Dynamics* Research

Fluid Dyn. Res. **48** (2016) 021402 (17pp) doi:10.1088/0169-5983/48/2/021402

Local equilibrium hypothesis and Taylor's dissipation law

Susumu Goto[1,3] **and J C Vassilicos**[2]

[1] Graduate School of Engineering Science, Osaka University, 1-3 Machikaneyama, Toyonaka, Osaka, 560-8531, Japan
[2] Department of Aeronautics, Imperial College, London, SW7 2AZ, UK

E-mail: goto@me.es.osaka-u.ac.jp and j.c.vassilicos@imperial.ac.jp

Received 26 August 2015, revised 1 December 2015
Accepted for publication 16 December 2015
Published 8 February 2016

Communicated by Christopher Keylock

Abstract

To qualitatively investigate the validity of Kolmogorov local equilibrium hypothesis and the Taylor dissipation law, we conduct direct numerical simulations of the three-dimensional turbulent Kolmogorov flow. Since strong scale-by-scale (i.e. Richardson-type) energy cascade events occur quasi-periodically, the kinetic energy of the turbulence and its dissipation rate evolve quasi-periodically too. In this unsteady turbulence driven by a steady force, instantaneous values of the dissipation rate obey the scaling recently discovered in wind tunnel experiments (Vassilicos 2015 *Ann. Rev. Fluid Mech.* **47** 95–114) instead of the Taylor dissipation law. The Taylor dissipation law does not hold because the local equilibrium hypothesis does not hold in a relatively low wave-number range. The breakdown of this hypothesis is caused by the finite time needed for the energy at such large scales to reach the dissipative scale by the scale-by-scale energy cascade.

Keywords: turbulence, local equilibrium hypothesis, dissipation law, Kolmogorov flow

1. Introduction

1.1. Local equilibrium hypothesis

The theory and modelling of turbulence have been developed on the basis of the so-called local equilibrium hypothesis. This hypothesis is explained, for example, in the introduction (on page 19) of the textbook of Tennekes and Lumley (1972) as follows:

[3] Author to whom any correspondence should be addressed.

> 'Since small-scale motions tend to have small time scales, one may assume that these motions are statistically independent of the relatively slow large-scale turbulence and of the mean flow. If this assumption makes sense, the small-scale motion should depend only on the rate at which it is supplied with energy by the large-scale motion and on the kinematic viscosity. It is fair to assume that the rate of energy supply should be equal to the rate of dissipation, because the net rate of change of small-scale energy is related to the time scale of the flow as a whole. The net rate of change, therefore, should be small compared to the rate at which energy is dissipated. This is the basis for what is called Kolmogorov's universal equilibrium theory of the small-scale structure.'

The main aim of the present study is to quantitatively examine whether or not this local equilibrium hypothesis holds. For this purpose, let us first describe the hypothesis unambiguously. We denote the energy spectrum by $E(k, t)$, with k and t being the wave number and time. Then, the kinetic energy $K^{>}(k, t)$ and its dissipation rate $\epsilon^{>}(k, t)$ per unit time in wave numbers larger than k are expressed in terms of $E(k, t)$ as

$$K^{>}(k, t) = \int_k^\infty E(k', t)\, \mathrm{d}k' \tag{1}$$

and

$$\epsilon^{>}(k, t) = 2\nu \int_k^\infty k'^2 E(k', t)\, \mathrm{d}k', \tag{2}$$

respectively. In (2), ν is the kinematic viscosity of the fluid. Then, we obtain

$$\frac{\partial K^{>}}{\partial t} = \Pi - \epsilon^{>} \tag{3}$$

by integrating the energy equation

$$\frac{\partial E}{\partial t} = -\frac{\partial \Pi}{\partial k} - 2\nu k^2 E + P, \tag{4}$$

over the wave-number range $[k, \infty)$. In the above equations, $\Pi(k, t)$ and $P(k, t)$ denote the energy flux function and the the power of the external force, respectively; and we have assumed that $P(k, t)$ has non-zero values only in a very low wave-number range. The local equilibrium hypothesis (see figure 1) implies the following: if the temporal evolution of $K^{>}(k, t)$ is sufficiently slow (more precisely, $|\partial K^{>}/\partial t| \ll \epsilon^{>}$), it follows that

$$\Pi(k, t) \approx \epsilon^{>}(k, t). \tag{5}$$

Equation (5) is a concrete expression of the local equilibrium hypothesis, and we examine the validity or invalidity of the hypothesis through (5).

The local equilibrium hypothesis is important for the following two reasons. First, it provides the basis for the Kolmogorov (1941a) similarity hypotheses. It is reasonable to assume that the statistics of turbulence at sufficiently small scales (i.e. for sufficiently high wave numbers) are determined by $\Pi(k, t)$ and ν. Therefore, if (5) holds for such high wave numbers, this may lead to the similarity hypothesis that the small-scale statistics are determined by the energy dissipation rate ϵ and ν. By the way, it is perfectly possible that a local equilibrium (5) can exist even when there are statistical dependencies between large-scale energetic motions and small-scale turbulence such as the dependencies discovered by

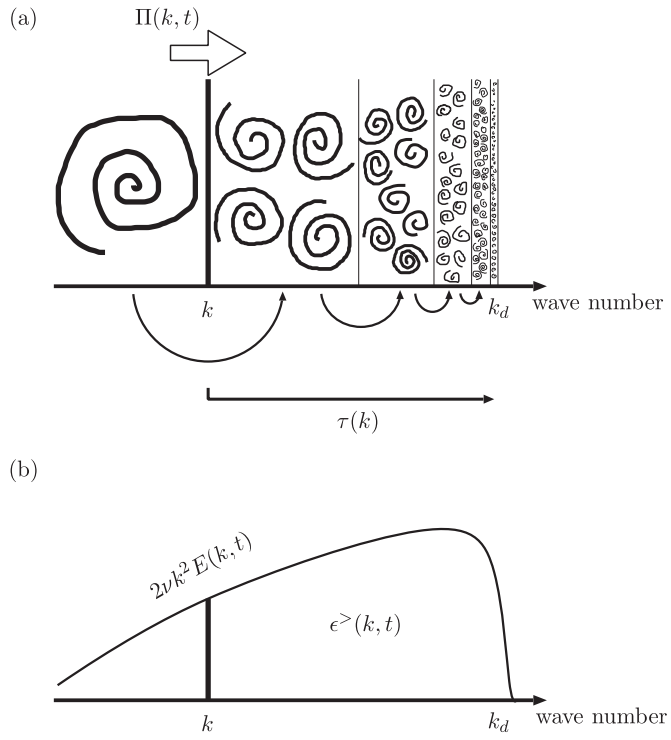

Figure 1. (a) The energy flux function $\Pi(k, t)$ denotes the energy supply per unit time to vortices smaller than k^{-1}. The time scale for the scale-by-scale energy cascade to reach the dissipative wave number k_d is denoted by $\tau(t)$. (b) Energy dissipation spectrum, $2\nu k^2 E(k, t)$. $\epsilon^>$ is the energy dissipation rate due to the molecular viscosity in the wave-number range $[k, \infty)$. The local equilibrium hypothesis requires the instantaneous balance between $\Pi(k, t)$ and $\epsilon^>(k, t)$. Therefore, this hypothesis holds only when $\tau(k)$ is much shorter than the time scale T_K of the temporal variation of the energy $K^>$ in eddies smaller than k^{-1}. Our DNS shows that T_K is of the order of $10\langle T\rangle$ where $\langle T\rangle$ is the mean turnover time of the largest eddies.

Praskovsky *et al* (1993). We do not study statistical dependencies such as those of Praskovsky *et al* (1993) in this paper.

Secondly, the hypothesis gives the basis of the Taylor (1935) dissipation law[3]. Here, we emphasise that, to justify the law, we must assume the validity of (5) even for $k \to L^{-1}$ with L being the integral length (as was argued in detail by Vassilicos 2015). Equation (2) leads to

$$\epsilon^>(k, t) \to \epsilon(t) \qquad (\text{as} \quad k \to L^{-1}). \tag{6}$$

On the other hand, $\Pi(L^{-1}, t)$, which is the loss rate of the energy of the flow at scales larger than $L(t)$, may be estimated as

[3] Indeed it was Kolmogorov (1941b) who gave a first derivation of the dissipation law (8), although Taylor (1935) wrote down the formula for the first time. Equation (8) may be therefore called the Taylor–Kolmogorov dissipation law, but for brevity we call it the Taylor law in this paper.

$$\Pi(k,\, t) \propto \frac{u'(t)^3}{L(t)} \qquad (\text{for} \quad k \approx L^{-1}). \tag{7}$$

Note that (7) is indeed a good estimate as discussed in section 3.6 of this paper on the basis of figure 9(a). Here, $u'(t)$ is defined so that the kinetic energy $K(t)$ of the fluid per unit mass is expressed as $K(t) = 3u'(t)^2/2$. Therefore, under the assumption that (5) holds even for k $\approx L^{-1}$, we obtain

$$\epsilon(t) \propto \frac{u'(t)^3}{L(t)}, \tag{8}$$

which we call the Taylor dissipation law. This law is the foundation of many statistical theories of turbulence, since it gives the estimation of $\epsilon(t)$, which is the key quantity of Kolmogorov's similarity hypothesis, just in terms of easily-measurable quantities, $u'(t)$ and $L(t)$.

1.2. Invalidity of (8)

However, the recent intensive experiments (Vassilicos 2015) of grid turbulence clearly showed that there exists a region in the decaying turbulence where (8) does not hold. This discovery casts doubt on the foundation of previous turbulence theories and modelling. More concretely, their experiments showed that the instantaneous value of the energy dissipation rate $\epsilon(t)$ obeys, instead of (8),

$$\epsilon(t) \propto \frac{Re_0^{p/2}}{R_\lambda(t)^q} \frac{u'(t)^3}{L(t)} \tag{9}$$

with constants $p \approx 1$ and $q \approx 1$. In (9), $Re_0 = U_0 L_0/\nu$ is a global Reynolds number based on a velocity U_0 and a length scale L_0 characterising the initial condition, and

$$R_\lambda(t) = \frac{u'(t)\lambda(t)}{\nu}. \tag{10}$$

is the instantaneous value of the Reynolds number based on $u'(t)$ and the Taylor length $\lambda(t)$. If we choose the values of $p = q = 1$, then using the relation

$$\epsilon(t) \propto \nu \frac{u'(t)^2}{\lambda(t)^2}, \tag{11}$$

we may reduce (9) to

$$\epsilon(t) \propto U_0 L_0 \frac{u'(t)^2}{L(t)^2}. \tag{12}$$

Although the new law (9) of dissipation has been supported by a considerable number of experiments (see Vassilicos 2015 and references therein), there is also experimental evidence (see figure 4 in Vassilicos 2015, for example) and a theoretical prediction (Meldi *et al* 2014) that (8) recovers in the further downstream decaying turbulence. It is therefore important to shed some light on the conditions for the validity and/or invalidity of (8).

Note that the energy spectrum is a power-law with exponent very close to $-5/3$ in the region of the turbulent flows where laboratory experiments have revealed the scaling (12). This is very different from the transients studied by Bos *et al* (2012) and Thalabard *et al* (2015) where the power law exponents of the energy spectrum are significantly smaller than $-5/3$.

1.3. Purpose

In the present study, we aim to revealing the cause of the invalidity of (8) by quantitatively examining (5) to see the condition under which the local equilibrium hypothesis holds. We also clarify the physics leading to the invalidity of the hypothesis.

For this purpose, we conduct direct numerical simulations (DNS) of turbulence at high Reynolds numbers, for which we can precisely evaluate instantaneous values of $\Pi(k, t)$ and $\epsilon^{>}(k, t)$.

In the following sections, we investigate the statistics of turbulence in a periodic cube, since we can numerically realise turbulence at sufficiently high Reynolds numbers under such simple boundary conditions. However, the DNS of decaying turbulence in a periodic cube is not necessarily easy, although we verified (12) by using the DNS of such turbulence (Goto and Vassilicos 2015). This is because it is unclear how to set up a natural initial condition and because the integral length grows indefinitely while the Reynolds number decreases in freely decaying turbulence. In contrast, it is easier to conduct DNS of forced turbulence in a periodic cube at higher Reynolds numbers. Interestingly, our recent studies (Yasuda *et al* 2014, Goto *et al* 2016, Goto and Vassilicos 2015) showed that turbulence driven by a steady force is not steady but quasi-periodic; and that such unsteadiness does lead to the invalidity of the dissipation law (8). In the present study, we examine the validity of the local equilibrium hypothesis with the help of DNS of turbulence driven by a simple steady force.

2. Direct numerical simulation

We numerically solve the equation of continuity, for the velocity field $\boldsymbol{u}(\boldsymbol{x}, t)$,

$$\boldsymbol{\nabla} \cdot \boldsymbol{u} = 0, \tag{13}$$

and the Navier–Stokes equation

$$\frac{\partial \boldsymbol{u}}{\partial t} + \boldsymbol{u} \cdot \boldsymbol{\nabla}\boldsymbol{u} = -\frac{1}{\rho}\,\boldsymbol{\nabla} p + \nu\,\nabla^2 \boldsymbol{u} + \boldsymbol{f} \tag{14}$$

under periodic boundary conditions (with the period of L_b) in three orthogonal directions. In (14), $p(\boldsymbol{x}, t)$ is the pressure field, and ρ is the constant density of the fluid.

In our DNS, we use an external force as simple as possible. The simplest spatially periodic force $\boldsymbol{f}(\boldsymbol{x})(=\boldsymbol{f}(x, y, z))$ may be

$$\boldsymbol{f} = f_0 \sin(2\pi y/L_\mathrm{b})\,\boldsymbol{e}_x, \tag{15}$$

which is expressed in terms of a single sinusoidal function. Here, f_0 is a constant, and $\boldsymbol{e}_x$ denotes the unit vector in the x direction. The flow driven by (15) is called the Kolmogorov flow.

When ν is sufficiently large, the flow driven by (15) is composed of a pair of steady vortex sheets. When ν is sufficiently small, turbulence is sustained with appropriate initial disturbance. The turbulence driven by (15) is statistically inhomogeneous and anisotropic at large scales. However, we emphasise that the energy equation (4), on which our theoretical arguments are based, holds even for inhomogeneous and anisotropic turbulence under periodic boundary conditions.

Our numerical schemes are the standard Fourier spectral method with the aliasing errors being removed by a phase-shift technique (see Canuto *et al* 2006 for more details of the numerical scheme). The temporal integration is made by using the 4th-order Runge–Kutta-Gill method with a time step satisfying the Courant–Friedrichs–Lewy condition.

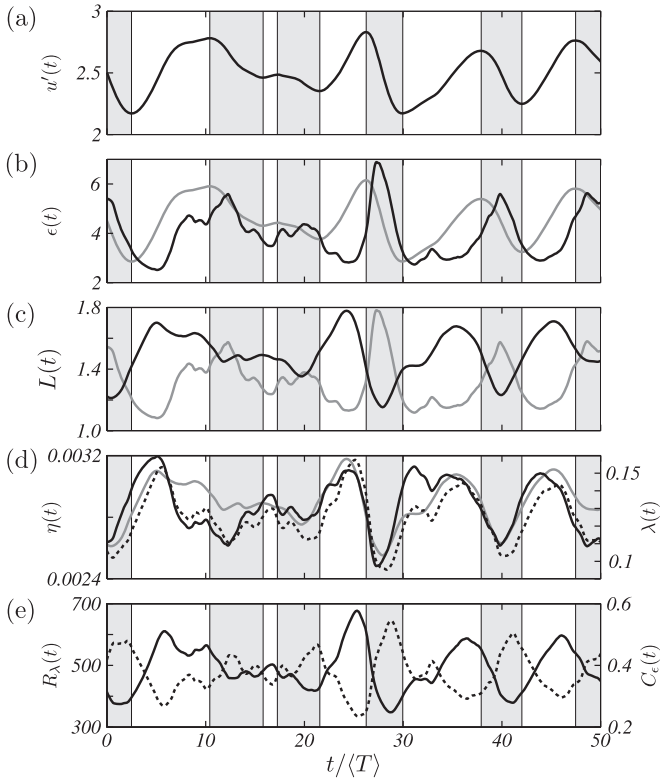

Figure 2. Temporal evolution of (a) $u'(t)$, (b) $\epsilon(t)$, (c) $L(t)$, (d) $\eta(t)$ (solid curve), $\lambda(t)$ (dotted), (e) $R_\lambda(t)$ (solid) and $C_\epsilon(t)$ (dotted). In (b), (c) and (d), $u'(t)$, $\epsilon(t)$ and $L(t)$ are replotted with a grey line, respectively, for reference. $\langle R_\lambda\rangle = 490$.

In our DNS, the integral length $L(t)$, Taylor length $\lambda(t)$ and Kolmogorov length $\eta(t)$ are evaluated by

$$L(t) = \frac{3\pi}{4}\int_0^\infty k^{-1}E(k,\,t)\,\mathrm{d}k/K(t), \tag{16}$$

$\lambda(t) = \sqrt{10\nu K(t)/\epsilon(t)}$ and $\eta(t) = \epsilon(t)^{-1/4}\nu^{3/4}$ with $K(t)$ and $\epsilon(t)$ being the spatial averages of the kinetic energy per unit mass and its dissipation rate, respectively. The following results are based on the DNS with up to $N^3 = 1024^3$ Fourier modes. The number of the modes was chosen, depending on the value of ν, so that $k_{\max}\eta(t)$ (with $k_{\max}$ being the highest resolved wave number, $\sqrt{2}N/3$) is always larger than 1.2.

3. Results

3.1. Quasi-periodic behaviour

Although the turbulent Kolmogorov flow is driven by the steady force (15), it behaves quasi-periodically in time (figure 2). The horizontal axis of figure 2 is the time normalised by the mean turnover time $\langle T\rangle = \langle L/u'\rangle$ of the largest eddies. Here, the brackets $\langle\cdot\rangle$ denote a temporal average. The initial transient evolution is not shown in this figure.

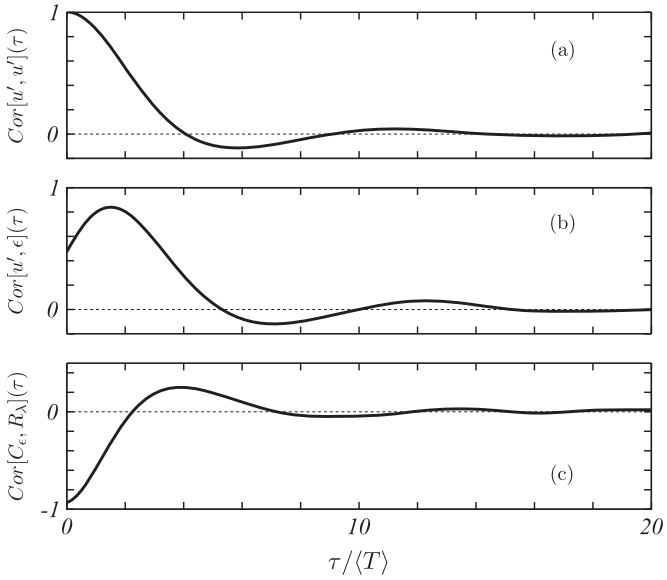

Figure 3. (a) Two-time auto-correlation function of $u'(t)$, and two-time correlation functions of (b) $u'(t)$ and $\epsilon(t)$ and (c) $C_\epsilon(t)$ and $R_\lambda(t)$. Statistics are taken over $2000\langle T \rangle$ for the turbulence at $\langle R_\lambda \rangle = 120$.

It is clear in figure 2(a) that $u'(t)$ evolves quasi-periodically with a period of about $10\langle T \rangle$. The amplitude of this oscillation is non-negligible; its standard deviation is about $0.08\langle u' \rangle$. As explained in the next subsection, this significant temporal oscillation of $u'(t)$ is caused by the quasi-periodic evolution of large-scale vortices, and leads to the temporal oscillation of other quantities with the same period but with different phases. To see the phase difference, the local extremes of $u'(t)$ are indicated by vertical lines in figure 2. For example, the temporal evolution of $\epsilon(t)$ is delayed from $u'(t)$ with a time lag of about $\langle T \rangle$ (figure 2(b)); whereas $\epsilon(t)$ and the integral length $L(t)$ are approximately in anti-phase (figure 2(c)), and equivalently $L(t)$ and the Kolmogorov length $\eta(t) = \epsilon(t)^{-1/4}\nu^{3/4}$ are approximately in phase (figure 2(d)). However, a close inspection of figure 2(d) shows that the synchronisation of $L(t)$ and the Taylor length $\lambda(t)$ is significantly stronger than that of $L(t)$ and $\eta(t)$. More quantitatively, $L(t)$ and $\lambda(t)$ oscillate with a standard deviation of about one tenth of their means, while the standard deviation of the oscillation of $L(t)/\lambda(t)$ is as small as $0.05\langle L/\lambda \rangle$. Furthermore, the time-scale of the oscillation of $L(t)/\lambda(t)$ is shorter than that ($\approx 10\langle T \rangle$) of $L(t)$ and $\lambda(t)$. This weak temporal variation of $L(t)/\lambda(t)$ contrasts with the fact that $R_\lambda(t)$ changes significantly (with a standard deviation of about $0.15\langle R_\lambda \rangle$) in time (figure 2(e)). Recall (11) to note that the constancy of $L(t)/\lambda(t)$ implies that $\epsilon(t)$ is proportional to $u'(t)^2/L(t)^2$ as in (12). We will return to this point in section 3.3.

In figure 2, we show the temporal evolution during $50\langle T \rangle$ of turbulence at a high Reynolds number $\langle R_\lambda \rangle = 490$. By conducting a much longer simulation over $2000\langle T \rangle$ at lower Reynolds number $\langle R_\lambda \rangle = 120$, we have verified that the observed phase deference between the quantities does not drift in time. More quantitatively, we show the two-time correlation functions of two quantities $A(t)$ and $B(t)$,

$$\mathrm{Cor}[A,\,B](\tau) = \frac{\langle (A(t) - \langle A\rangle)(B(t+\tau) - \langle B\rangle)\rangle}{\sqrt{\langle (A(t) - \langle A\rangle)^2\rangle \langle (B(t) - \langle B\rangle)^2\rangle}}, \tag{17}$$

for $(A,\,B) = (u',\,u')$, $(u',\,\epsilon)$ and $(C_\epsilon,\,R_\lambda)$ in figure 3. Figures 3(b) and (c) show that the time lag (about $1.5\langle T\rangle$) between $u'(t)$ and $\epsilon(t)$ (figure 2(b)) and the anti-phase behaviour of $C_\epsilon(t)$ and $R_\lambda(t)$ (figure 2(e)) are robust. In addition, figure 3(a) quantifies the period of the cycle to be $11\langle T\rangle$ for this Reynolds number. It seems that these features are independent of the Reynolds number, but quantitative verification of this independence is left for future study.

3.2. Scale-by-scale energy cascade

We can explain the quasi-periodic behaviour of $u'(t)$ and $\epsilon(t)$ observed in figure 2 in terms of the scale-by-scale (Richardson-type) cascade of energy. The following is a summary of the observations demonstrated by Goto *et al* (2016). First, the turbulence is composed of a hierarchy of anti-parallel vortex tubes with various sizes, and smaller-scale vortex tubes are created by stretching in strain fields around larger-scale vortex tubes. Secondly, the scale-locality of the vortex stretching was quantitatively verified; namely, the energy cascade occurs in a scale-by-scale manner[4].

On the basis of these observations, the quasi-periodic evolution of $u'(t)$ and $\epsilon(t)$ may be described as follows. (i) The external force (15) inputs the energy to create large-scale vortex tubes in the vortex sheets. During this period, the kinetic energy $K(t) = 3u'(t)^2/2$ significantly increases. (ii) Once the energetic large-scale vortex tubes are established, scale-by-scale energy cascade events start to create smaller-scale vortex tubes. During this period, $\epsilon(t)$ increases significantly. (iii) Since the smallest-scale vortices become energetic, $\epsilon(t)$ dominates over the power of the external force, and the turbulence decays. During this period, both $K(t)$ and $\epsilon(t)$ decrease significantly. Then, the entire system becomes quiescent. (i′) Finally, the power of the external force dominates over $\epsilon(t)$ to re-create the large-scale vortex tubes and re-start the cycle all over again.

In summary, the quasi-periodic temporal oscillations of $u'(t)$ and $\epsilon(t)$ correspond to the cyclic events of the scale-by-scale cascade of energy. This conclusion is drawn from qualitative observations of the energy cascade (Goto *et al* 2016). It is therefore an important future study to examine the temporal evolution of production rates of the (scale-by-scale) vorticity and rate-of-strain.

Incidentally, Goto *et al* (2016) also verified that, if the forcing is kept the same, the period of the quasi-periodic behaviour is independent of Reynolds number. This is consistent with the classical view of the energy cascade. As mentioned above, since the creation of smaller-scale vortices occurs in a scale-by-scale manner, the increase of the Reynolds number only adds some steps of the cascade at smaller scales. Therefore, such an increase of the Reynolds number may not affect the temporal evolution of the largest vortices which determine $u'(t)$.

[4] Here, as well as in our previous studies, we use the words 'Richardson cascade' to denote the scale-by-scale energy cascade as described in Richardson (1922)'s famous verse, and the 'Richardson–Kolmogorov cascade' to denote a Richardson cascade with Kolmogorov (1941a) local equilibrium throughout the entire inertial range.

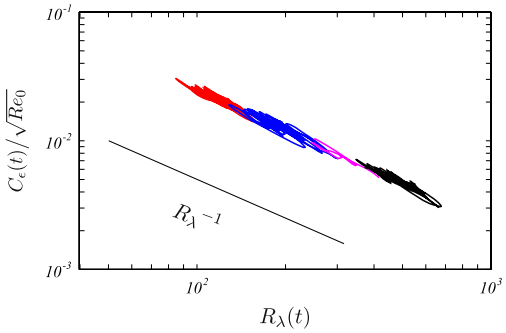

Figure 4. Verification of (12). We plot $C_\epsilon(t)$ divided by $\sqrt{Re_0}$ as a function of $R_\lambda(t)$ for different time-averaged Reynolds numbers: $\langle R_\lambda \rangle = 120$ (red), 190 (blue), 310 (purple) and 490 (black).

3.3. Dissipation laws

We return to figure 2(e), which shows that the normalised dissipation rate

$$C_\epsilon(t) = \frac{\epsilon(t)}{u'(t)^3/L(t)} \tag{18}$$

changes significantly in time and is in anti-phase with $R_\lambda(t)$; see also figure 3(c). If the Taylor dissipation law (8) was valid, $C_\epsilon(t)$ would have been a constant independent of $R_\lambda(t)$. The observations clearly violate (8). We emphasise that the violation of (8) is not a transient because the quasi-periodic behaviour (figure 2) is permanent.

Note that the anti-phase evolutions of $C_\epsilon(t)$ and $R_\lambda(t)$ support (9) with $q = 1$. To verify (12), that is (9) with $p = q = 1$, we plot $C_\epsilon(t)/\sqrt{Re_0}$ in figure 4 as a function of $R_\lambda(t)$ for four cases with four different values of $\langle R_\lambda \rangle$ (i.e. with four different values of ν). Here, to estimate $Re_0 = U_0 L_0/\nu$, we have taken $U_0 = \langle u' \rangle$ and $L_0 = \langle L \rangle$. Figure 4 shows that the dissipation law (12) gives a fairly good approximation of $\epsilon(t)$ not only in the decaying periods of the turbulence, but also in its building-up periods.

Incidentally, Goto and Vassilicos (2015) demonstrated that (12) holds in DNS turbulence driven by a different external force than the one used here. This suggests that (12) may be valid for a wide range of forcings. Recall that the turbulence examined in this study is inhomogeneous and anisotropic at large scales and that $u'(t)$ and $L(t)$ are evaluated through the three-dimensional energy spectrum $E(k, t)$. However, in many different kinds of laboratory experiments and DNS with different levels of inhomogeneity and anisotropy, (12) is quite robustly supported irrespective of the precise way these quantities are defined (Valente and Vassilicos 2014, Dairay *et al* 2015, Vassilicos 2015).

As mentioned in the introduction, the violation of (8) implies the invalidity of either (5) or (7). Since the latter is valid (see figure 9(a) in section 3.6), the violation of (8) implies the invalidity of the local equilibrium hypothesis (5).

3.4. Invalidity of the local equilibrium hypothesis for low wave numbers

In this subsection, we directly verify that the local equilibrium hypothesis does not hold in a low wave-number range. We plot in figure 5 the temporal evolution of $\epsilon^>(k, t)$ (with thick grey lines) and the evolution of $\Pi(k, t)$ (with thin black lines) for the run at $\langle R_\lambda \rangle = 490$. Recall that if the local equilibrium hypothesis is valid, (5) holds. Figure 5 clearly shows that

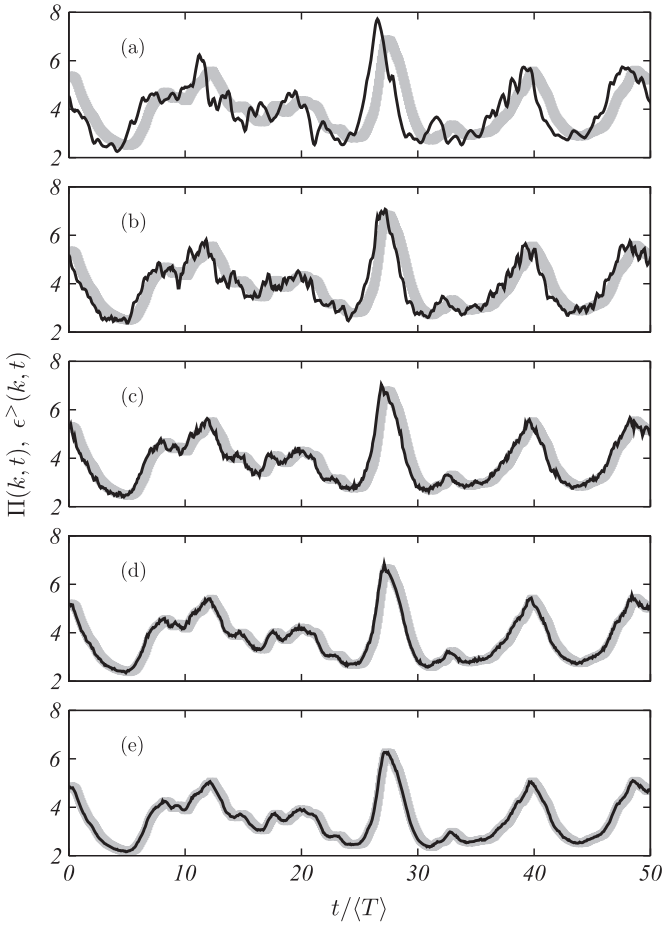

Figure 5. Temporal evolution of $\epsilon^{>}(k,\ t)$ (thick grey lines) and $\Pi(k,\ t)$ (thin black lines) for (a) $k = 2k_{\mathrm{f}}$, (b) $4k_{\mathrm{f}}$, (c) $8k_{\mathrm{f}}$, (d) $16k_{\mathrm{f}}$ and (e) $32k_{\mathrm{f}}$. $\langle R_{\lambda}\rangle = 490$.

(5) gives a good approximation for high wave numbers (say, $k \gtrsim 20k_{\mathrm{f}}$), but not for low k. Here, $k_{\mathrm{f}}\,(=1)$ denotes the forcing wave number. It is this invalidity of (5), i.e. the invalidity of the local equilibrium hypothesis, in a low wave-number range that is the cause of the violation of the Taylor dissipation law (8).

Figure 5 also shows that the peaks of $\Pi(k,\ t)$ appear at later times for higher wave numbers. Hence, given that $\epsilon^{>}(k,\ t)$ are synchronised for all k and therefore also synchronised with $\epsilon\ (k,\ t)$ (see the next paragraph), the phase of $\Pi(k,\ t)$ approaches that of $\epsilon\ (k)$ as the wave number increases. This is consistent with the argument on the energy cascade in section 3.2. Recall that the quasi-periodic behaviour of this turbulence is due to cyclic events of strong energy cascade, and that the cascade (i.e. the creation of smaller-scale eddies) occurs in a scale-by-scale manner. These are the reasons why the temporal evolution of $\Pi(k,\ t)$ is more delayed, and its time lag with $\epsilon\ (t)$ therefore reduced, for higher wave numbers. It is also seen in this figure that it takes a few eddy turnover times for the energy to cascade from the largest scale to the dissipative scale. Namely, the local equilibrium hypothesis for a low wave number k is violated because it takes a non-negligible time (compared with the variation time

scale T_K of $K^>(k, t)$) for the energy to cascade from the scale k^{-1} to the dissipative scale $k_\mathrm{d}{}^{-1}$ (figure 1); a more quantitative argument is given in the next subsection.

Incidentally, it is also seen in figure 5 that $\epsilon^>(k, t)$ at different wave numbers are approximately in phase. This is trivial for lower wave numbers because $\epsilon^>(k, t) \approx \epsilon(t)$. For higher k, on the other hand, $\epsilon^>(k, t) \approx \Pi(k, t)$; and there are only small time lags between $\Pi(k, t)$, as observed in figure 5, in a high wave-number range because cascading time scale gets smaller for higher k. These are the reasons why $\epsilon^>(k, t)$ evolve together for different k.

Our conclusion in this subsection is in agreement with Yoshizawa (1994) who predicted that the non-equilibrium is more marked at lower than at higher wave numbers. However, Yoshizawa (1994)'s non-equilibrium prediction for the energy spectrum implies a dissipation coefficient C_ϵ which is different from the one observed in the present and previous (Goto and Vassilicos 2015) DNS and in previous laboratory experiments (Dairay *et al* 2015, Vassilicos 2015). By integrating Yoshizawa's energy spectrum (equation (43) in his paper) one obtains

$$C_\epsilon \sim \left[1 + \mathrm{sgn}\left(\frac{D\epsilon}{Dt}\right) C_y \left(\frac{L}{L_p}\right)^{2/3}\right]^{-3/2} \tag{19}$$

where C_y is a positive non-dimensional constant and L_p is the non-equilibrium length-scale which he defines as $L_p = \epsilon^2/(D\epsilon/Dt)^{3/2}$ and shows that $L_p > L$. Note that his prediction (19) for C_ϵ (which he actually did not include in his paper) is different from (12).

3.5. Validity condition of the local equilibrium hypothesis

We have observed in the previous subsection that, at $\langle R_\lambda \rangle = 490$, the local equilibrium hypothesis gives a good approximation for wave numbers k higher than about $20k_\mathrm{f}$, but not for $k \lesssim 20k_\mathrm{f}$. In this subsection, we determine the Reynolds-number dependence of the wave-number condition for the validity of this hypothesis.

We plot $\langle \Pi \rangle / \langle \epsilon \rangle$ in figure 6(a) for this Reynolds number. Defining the inertial range as the wave number range with $\langle \Pi \rangle \approx \langle \epsilon \rangle$, figure 6(a) indicates that the inertial range is $k \lesssim 0.1 \langle \eta \rangle^{-1}$ ($k \lesssim 20k_\mathrm{f}$) for this Reynolds number. Therefore, one would conclude that the local equilibrium hypothesis is invalid in the entire inertial range and valid in the dissipative range. However, the situation is not so simple.

In figure 6(b) we plot $\langle \Pi \rangle / \langle \epsilon \rangle$ for a lower Reynolds number, i.e. $\langle R_\lambda \rangle = 190$. Comparing figures 6(a) and (b), it is clear that $\langle \Pi \rangle / \langle \epsilon \rangle$ as a function of the normalised wave number $k \langle \eta \rangle$ is independent of $\langle R_\lambda \rangle$. This implies that the inertial range as defined here (i.e. as a time-average concept for an unsteady turbulence, not an instantaneous concept) is always $k \lesssim 0.1 \langle \eta \rangle^{-1}$ irrespective of $\langle R_\lambda \rangle$.

On the other hand we also provide figure 7, which is similar to figure 5, as an instantaneous check of (5) for this lower Reynolds number. This figure indicates that the local equilibrium hypothesis also holds for $k \gtrsim 20k_\mathrm{f}$ for this lower $\langle R_\lambda \rangle$ as it does for the higher $\langle R_\lambda \rangle$ in figure 5. For a more quantitative comparison of the two terms in (5), we plot in figure 8 the temporal average of the difference $|\Pi(k, t) - \epsilon^>(k, t)|$ normalised by the average of $\epsilon^>(k, t)$ as a function of k for different Reynolds numbers. Figure 8 shows that the average quantity plotted collapses better as a function of k/k_f than as a function of $k \langle \lambda \rangle$ and that it drops below 5% at k larger than about $15k_\mathrm{f}$. (Note that the collapse is not perfect at k smaller than $15k_\mathrm{f}$ in figure 8(a) as a non-negligible systematic variation remains.) On the basis of figures 5, 7 and 8, we may conclude that the local equilibrium hypothesis holds on average for $k \gtrsim 20k_\mathrm{f}$ irrespective of the Reynolds number.

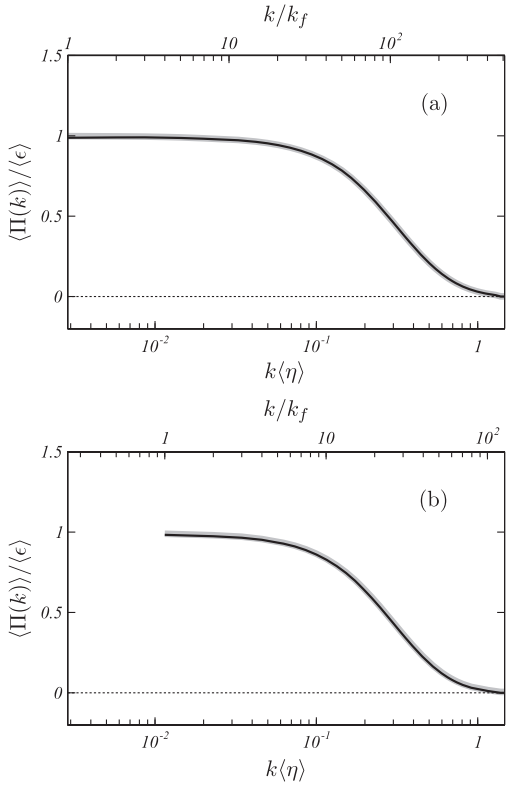

Figure 6. Temporal average $\langle\Pi(k)\rangle$ of the flux function normalised by the averaged energy dissipation rate $\langle\epsilon\rangle$. Grey thick line denotes $\langle\epsilon^{>}(k)\rangle/\langle\epsilon\rangle$. (a) $\langle R_\lambda\rangle = 490$ and (b) 190.

This conclusion is consistent with the argument in the previous subsection. That is, the invalidity of the local equilibrium hypothesis is due to the fact that it takes a finite time for the energy to cascade from a low wave number to k_d. More concretely, let $\tau(k)$ be an average time for the energy at a given wave number k to cascade to the dissipation range. If $\tau(k)$ for a given wave number k is not negligible compared to the time scale $T_K(k)$ of the variation of $K^{>}(k, t)$, then the local equilibrium hypothesis is invalid for such a wave number k. Note that $T_K(k)$ is always of the order of $\langle L\rangle/\langle u'\rangle$ irrespective of k and average Reynolds number. In other words, for a wave number k which satisfies

$$\tau(k) \ll \langle L\rangle/\langle u'\rangle, \tag{20}$$

the local equilibrium hypothesis holds. Estimating $\tau(k) \approx \langle\epsilon\rangle^{-1/3}k^{-2/3}$ (note the use of the time-averaged and not the instantaneous dissipation rate) and using the Taylor dissipation law (8) for the average dissipation rate (for which it holds as shown by Goto and Vassilicos 2015), we conclude that for $k \gg \langle L\rangle^{-1} \approx k_\mathrm{f}$ the hypothesis is valid. This argument suggests that, for high enough average Reynolds number, there exists a range of wave numbers within the inertial range (defined as a time-average concept) where the local equilibrium hypothesis might, on average, hold. (We will present a more rigorous and more general argument concerning this point in a forthcoming publication.)

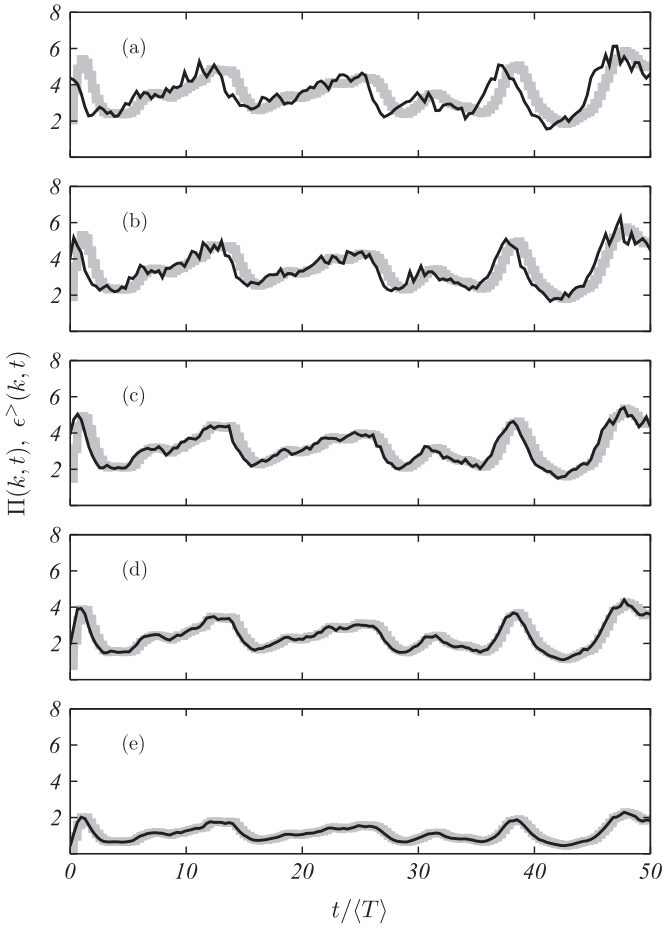

Figure 7. Same as figure 5, but for a lower Reynolds number, $\langle R_\lambda \rangle = 190$.

3.6. Scaling of the energy flux

In this last subsection, we briefly investigate the scaling of $\Pi(k, t)$. We plot in figure 9 the temporal evolution of $\Pi(k, t)$ together with those of $\epsilon(t)$ and

$$X(t) = C_X \frac{u'(t)^3}{L(t)} \tag{21}$$

for five different wave numbers. Here we set $C_X = 0.38$.

We can see in figure 9(a) that, for $k \approx k_f$ ($\approx L^{-1}$), the energy flux $\Pi(k, t)$ is well approximated by $X(t)$. In other words, (7) is indeed valid for $k \approx k_f$.

However, for higher wave numbers (say, $k \gtrsim 20k_f$), the phase of $\Pi(k, t)$ is delayed with a finite lag from $X(t)$. This is because it takes a finite time for the energy to cascade from k_f to such a higher wave number. For the same reason, as k increases, the phase of $\Pi(k, t)$ approaches that of $\epsilon(t)$. This synchronisation of $\Pi(k, t)$ and $\epsilon(t)$ at higher wave-numbers is also clear in figures 5 and 7. Recall that, as discussed in the last paragraph of section 3.4, $\epsilon^{>}(k, t)$ and $\epsilon(t)$ are approximately in phase. In conclusion, $\Pi(k, t)$ for $k \gtrsim 20k_f$ is not scaled as $X(t)$, but it obeys the same scaling as $\epsilon(t)$. Note that this is the case even in what we term

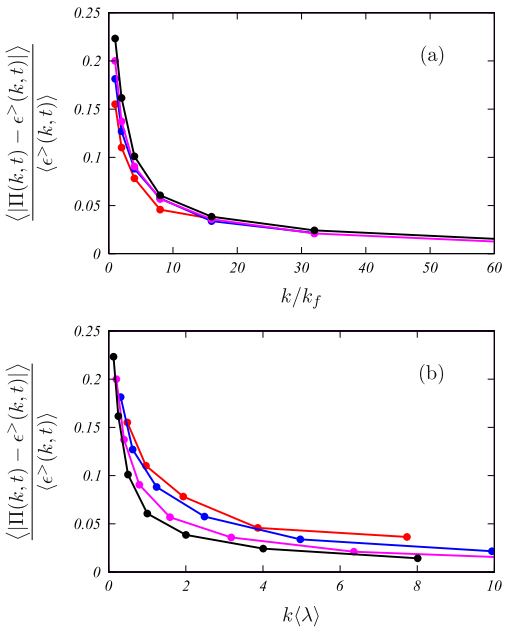

Figure 8. Difference between $\Pi(k,\ t)$ and $\epsilon^{>}(k,\ t)$, which is required to be 0 by (5), as a function of the wave number k normalised by (a) the forcing wave number k_{f} and by (b) the temporally averaged Taylor length $\langle\lambda\rangle$. Different colours are for different time-averaged Reynolds numbers: $\langle R_\lambda\rangle = 120$ (red), 190 (blue), 310 (purple) and 490 (black).

the inertial range if the Reynolds number is sufficiently high as wave numbers ($k \gtrsim 20k_{\mathrm{f}}$) will exist in such a wide range. This conclusion on the scaling of $\Pi(k,\ t)$ is consistent with the observations of Goto and Vassilicos (2015).

Incidentally, we can reconfirm, in figure 9, that $\epsilon\,(t)$ (dotted lines) is delayed from $X(t)$ (thick grey lines), and that (8) is indeed invalid.

4. Concluding remarks

The energy dissipation rate $\epsilon\,(t)$ of the turbulent Kolmogorov flow driven by the steady force (15) oscillates quasi-periodically in time with a significant amplitude and a period of about $10\langle T\rangle$ (figures 2 and 3(a)). The instantaneous value of $\epsilon\,(t)$ obeys (9) with $p = q = 1$ instead of the Taylor dissipation law (8) as shown in figure 4.

The Taylor dissipation law (8) requires that the local equilibrium hypothesis is valid even for low wave numbers $k \approx L^{-1}(\approx k_{\mathrm{f}})$. However, our examination (figures 5, 7 and 8) of the local equilibrium hypothesis expressed in the form of (5) shows that this hypothesis holds only for $k \gtrsim 20k_{\mathrm{f}}$. Namely, the breakdown of this hypothesis in the lower part ($k \lesssim 20k_{\mathrm{f}}$) of the inertial range (which we defined in a time-average sense, see figure 6) explains why (8) does not hold. As explained in sections 3.4 and 3.5, the physics underpinning the breakdown of this hypothesis in that lower wave-number range is the scale-by-scale cascade of energy and the cascade time-lag that it naturally implies. Consistent with these cascade time-lag physics, $\Pi(k,\ t)$ scales as $u'(t)^3/L(t)$ at $k \approx k_{\mathrm{f}}$ (figure 9) but is proportional to $\epsilon\,(t)$, and therefore scales as in (12) at $k \gtrsim 20k_{\mathrm{f}}$.

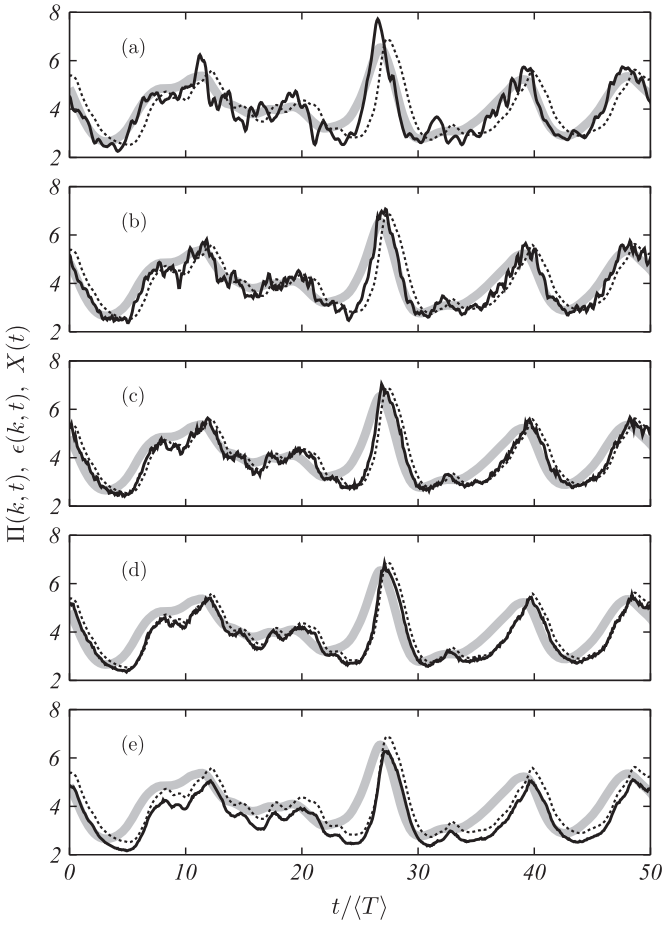

Figure 9. Temporal evolution of $\Pi(k,\ t)$ (thin black lines), $\epsilon\ (t)$ (dotted lines) and $X\,(t)$ (thick grey lines) for (a) $k = 2k_{\mathrm{f}}$, (b) $4k_{\mathrm{f}}$, (c) $8k_{\mathrm{f}}$, (d) $16k_{\mathrm{f}}$ and (e) $32k_{\mathrm{f}}$. $\langle R_\lambda\rangle = 490$.

The validity condition ($k \gtrsim 20k_{\mathrm{f}}$) of the local equilibrium hypothesis is likely to be the same even in the high Reynolds number limit for such forced, quasi-periodic, turbulence. This is because even if we increase the Reynolds number (i.e. decrease ν with a fixed force), only some steps of the scale-by-scale energy cascade at small length scales with shorter time scales are added; and because the period of the quasi-periodic behaviour seems to be independent of Reynolds number for a given forcing (Yasuda *et al* 2014, Goto *et al* 2016).

This paper's conclusions may well be general for forced turbulence in a periodic cube, since the quasi-periodic behaviour due to strong cascade events is observed in turbulences driven by different forces (Goto *et al* 2016). It is worth mentioning that such a cyclic behaviour is ubiquitous in many systems; for example, see the laboratory experiments on the von Kármán flow (Pinton *et al* 1999) and the DNS of turbulent homogeneous shear flow (Horiuti and Ozawa 2011).

It is also worth emphasising that, as demonstrated by Goto and Vassilicos (2015), the Taylor dissipation law (8) gives a good approximation for the long-time average of the dissipation rate in terms of $\langle L\rangle$ and $\langle u'\rangle$ for a forced turbulent flow in a periodic cube. This

implies that, if the period of the boundary condition in such forced turbulence was much longer than $\langle L \rangle$, then even the instantaneous values of $\epsilon(t)$ would obey (8). The reason for this is that the spatial average of a quantity over such a very large domain in such a flow is time-independent and therefore equal to its time average. However this is not the case in unforced decaying periodic turbulence and in spatially decaying turbulence such as can be found in grid-generated turbulent flows and turbulent wakes (see Goto and Vassilicos 2015, Dairay *et al* 2015 and Vassilicos 2015). The validity of the Taylor dissipation law (8) for instantaneous $\epsilon(t)$ in a very large domain of a turbulence forced over a length-scale much smaller than the size of that domain is consistent with the present conclusion that its invalidity is due to the quasi-cyclic scale-by-scale energy cascade. Indeed, in such a very large domain, various phases of the cyclic energy cascade will coexist thus yielding the average dissipation law (8) on an instantaneous basis. This can of course not happen in continuously decaying turbulence such as can be found in various free shear turbulent flows and grid-generated turbulence.

The scale-by-scale cascade physics which are the root cause of the invalidity of Taylor's dissipation law (8) must also hold or at least be related to the reason for the new dissipation law (9). Two important open questions therefore remain which we plan to address in future publications. First, we need to understand the mechanism which leads to the relatively abrupt passage from the new dissipation law (9) to Taylor's law (8) in the far downstream and long time turbulence decays. And secondly we need a theoretical derivation of the new dissipation law (9) for the wide range of turbulent flows where it appears to hold. Adopting the values $p = q = 1$ which are close to observations, (9) is reduced to (12) and relates $\epsilon(t)$ to the large-scale quantities $u'(t)$ and $L(t)$. This suggests some kind of balance between fluid motions at different scales. Therefore, the validity condition, which has been shown here, of the local equilibrium hypothesis as well as the observations concerning local equilibrium and non-equilibrium and scale-by-scale cascades may prove useful for the development of theoretical arguments leading to the new dissipation law.

Acknowledgments

This study is partially supported by JSPS Grants-in-Aid for Scientific Research 25249014 and 26630054 and by an ERC Advanced Grant (2013–2018).

References

Bos W J T, Connaughton C and Godeferd F 2012 Developing homogeneous isotropic turbulence *Physica* D **241** 232–6

Canuto C, Hussaini M Y, Quarteroni A and Zang T A 2006 *Spectral Methods* (Berlin: Springer)

Dairay T, Obligado M and Vassilicos J C 2015 Non-equilibrium scaling laws in axisymmetric turbulent wakes *J. Fluid Mech.* **781** 166–95

Goto S, Saito Y and Kawahara G 2016 Hierarchy of anti-parallel vortex tubes in turbulence at high Reynolds numbers (submitted)

Goto S and Vassilicos J C 2015 Energy dissipation and flux laws for unsteady turbulence *Phys. Lett.* A **379** 1144–8

Horiuti K and Ozawa T 2011 Multimode stretched spiral vortex and nonequilibrium energy spectrum in homogeneous turbulence *Phys. Fluids* **23** 035107

Kolmogorov A N 1941a The local structure of turbulence in incompressible viscous fluid for very large Reynolds numbers *Dokl. Akad. Nauk SSSR* **30** 301–5

Kolmogorov A N 1991 *Proc. R. Soc.* A **434** 9–13 (Engl. transl.)

Kolmogorov A N 1941b On the degeneration of isotropic turbulence in an incompressible viscous fluid *Dokl. Akad. Nauk SSSR* **31** 538–41
Kolmogorov A N 1991 *Selected Works of A. N. Kolmogorov* vol 1 (Berlin: Springer) pp 319–323 (Engl. transl.)
Meldi M, Lejemble H and Sagaut P 2014 On the emergence of non-classical decay regimes in multiscale/fractal generated isotropic turbulence *J. Fluid Mech.* **756** 816–43
Pinton J F, Holdsworth P C W and Labbé R 1999 Power fluctuations in a closed turbulent shear flow *Phys. Rev.* E **60** R2452–5
Praskovsky A A, Gledzer E B, Karyakin M Y and Zhou A Y 1993 The sweeping decorrelation hypothesis and energy-inertial scale interaction in high Reynolds number flows *J. Fluid Mech.* **248** 493–511
Richardson L F 1922 *Weather Prediction by Numerical Process* (Cambridge: Cambridge University Press)
Taylor G I 1935 Statistical theory of turbulence *Proc. R. Soc.* A **151** 421–44
Tennekes H and Lumley J L 1972 *A First Course in Turbulence* (Cambridge, MA: MIT Press)
Thalabard S, Nazarenko S, Galtier S and Medvedev S 2015 Anomalous spectral laws in differential models of turbulence *J. Phys.* A **48** 285501
Valente P C and Vassilicos J C 2014 The non-equilibrium region of grid-generated decaying turbulence *J. Fluid Mech.* **744** 5–37
Vassilicos J C 2015 Dissipation in turbulent flows *Ann. Rev. Fluid Mech.* **47** 95–114
Yasuda T, Goto S and Kawahara G 2014 Quasi-cyclic evolution of turbulence driven by a steady force in a periodic cube *Fluid Dyn. Res.* **46** 061413
Yoshizawa A 1994 Nonequilibrium effect of the turbulent-energy-production process on the inertial-range energy spectrum *Phys. Rev.* E **49** 4065–71